http://www.jstage.jst.go.jp/browse/biophysics

BIOPHYSICS

Vol. 9, pp. 21–29 (2013)
doi: 10.2142/biophysics.9.21

Expression, purification and biochemical characterization of the cytoplasmic loop of PomA, a stator component of the Na^+ driven flagellar motor

Rei Abe-Yoshizumi[1], Shiori Kobayashi[1], Mizuki Gohara[1], Kokoro Hayashi[2], Chojiro Kojima[2], Seiji Kojima[1], Yuki Sudo[1], Yasuo Asami[3] and Michio Homma[1]

[1]*Division of Biological Science, Graduate School of Science, Nagoya University, Chikusa-ku, Nagoya 464-8602, Japan*
[2]*Laboratory of Biophysics, Graduate School of Biological Sciences, Nara Institute of Science and Technology, 8916-5 Takayama, Ikoma, Nara 630-0192, Japan*
[3]*TA Instruments Japan, Inc., 5-2-4, Nishi-gotanda, Shinagawa-ku, Tokyo 141-0031, Japan*

Received December 20, 2012; accepted January 8, 2013

Flagellar motors embedded in bacterial membranes are molecular machines powered by specific ion flows. Each motor is composed of a stator and a rotor and the interactions of those components are believed to generate the torque. Na^+ influx through the PomA/PomB stator complex of *Vibrio alginolyticus* is coupled to torque generation and is speculated to trigger structural changes in the cytoplasmic domain of PomA that interacts with a rotor protein in the C-ring, FliG, to drive the rotation. In this study, we tried to overproduce the cytoplasmic loop of PomA (PomA-Loop), but it was insoluble. Thus, we made a fusion protein with a small soluble tag (GB1) which allowed us to express and characterize the recombinant protein. The structure of the PomA-Loop seems to be very elongated or has a loose tertiary structure. When the PomA-Loop protein was produced in *E. coli*, a slight dominant effect was observed on motility. We conclude that the cytoplasmic loop alone retains a certain function.

Abbreviations: PomA, Polar flagellar motility protein A; PomB, Polar flagellar motility protein B; PGB, peptidoglycan-binding; SDS-PAGE, sodium dodecyl sulfate-polyacrylamide gel electrophoresis; CD, circular dichroism

Corresponding author: Michio Homma, Division of Biological Science, Graduate School of Science, Nagoya University, Chikusa-ku, Nagoya 464-8602, Japan.
e-mail: g44416a@cc.nagoya-u.ac.jp

Key words: bacterial flagellum, ion-driven motor, protein interaction, stator

Many species of bacteria swim by rotating their helical flagella toward favorable stimuli in liquid environments. Previous studies have revealed that about 50 kinds of proteins are involved in the assembly and function of flagella[1,2]. Flagellar motors are molecular machines powered by an electrochemical potential gradient of specific ions across the membrane, and are classified according to the respective coupling ion. Some bacteria, such as *Escherichia coli* and *Salmonella enterica*, have motors driven by the H^+ motive force[3], while others, such as alkalophilic *Bacillus* and marine *Vibrio* species[4], have Na^+-driven motors. Each motor is composed of a stator and a rotor, and multiple stator units are anchored around the rotor. The torque generation that drives the rotor is coupled to the ion translocation through the stator complex[5,6].

The stator proteins of the *E. coli* H^+-driven motor have been identified as MotA and MotB, mutations in which exhibit a *mot*$^-$ phenotype with intact flagella but no ability to move[3]. The Na^+-driven stator of *Vibrio alginolyticus* is encoded by homologous genes called *pomA* and *pomB*[7]. PomA or MotA and PomB or MotB are integral membrane proteins having four and one transmembrane domains, respectively, and form ion-conducting complexes in the membrane[8,9]. The Na^+-conducting activity of the PomA/PomB

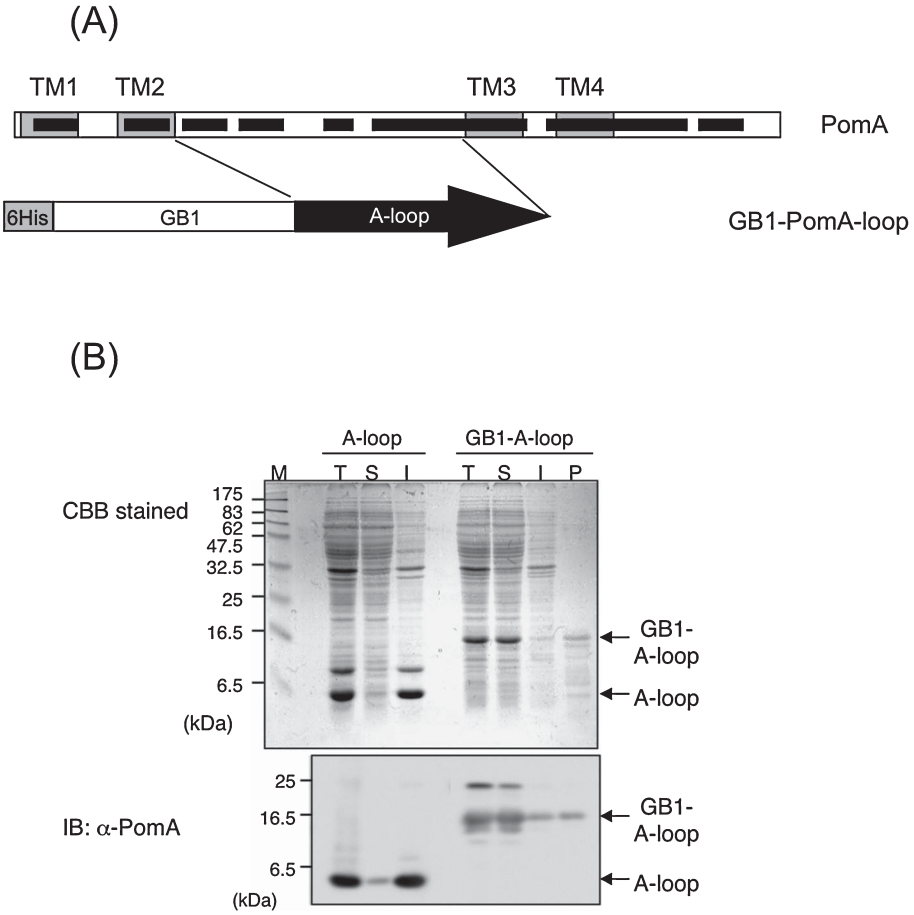

Figure 1 (A) Schematic diagram of PomA and the fusion construct of the PomA-Loop with GB1. (B) SDS-PAGE profiles of the PomA-Loop (A-loop) and the PomA-Loop fused with GB1 (GB1-A-loop). Proteins in the gels were stained with Coomassie Brilliant Blue (CBB), and were detected by immunoblotting (IB) using an anti-PomA antibody. M, T, S and I represent molecular size markers, total cell lysate, soluble fraction and insoluble fraction, respectively. P represents the fraction purified by a Ni-affinity column and an ion exchange column, Hitrap Q.

complex has been shown *in vitro* using reconstituted proteoliposomes[10]. PomB has a putative ion binding site, D24, in the transmembrane segment, a peptidoglycan-binding (PGB) domain at the C-terminus in the periplasmic region, and is attached to the peptidoglycan layer to support the motor[11,12]. In contrast, PomA has a C-terminal cytoplasmic tail with about 55 residues and a large cytoplasmic loop (the PomA-Loop) between the 2nd and 3rd transmembrane domains with about 95 residues (ca. 10 kDa) (Fig. 1)[13]. The loop region has been speculated to cause a conformational change induced by the ion binding that drives the rotor through its interaction with a rotor protein, FliG[14].

On the rotor side, three proteins, FliG, FliM and FliN, have been shown to be directly involved in torque generation[15,16]. They constitute the structure called the "C-ring" (about 300 Å in diameter) that is attached to the cytoplasmic side of the MS-ring[17,18]. The FliG/M/N complex is also called the "switch complex" because a mutation in any of them causes a defect in the regulation of rotational direction. Previous studies of the *E. coli* motor showed that FliG most closely participates in torque generation. As described above, interactions between the cytoplasmic loop of PomA (or MotA) and FliG are important for torque generation. Genetic studies, as described below, show that the C-terminal domain of FliG is responsible for such interactions, and crystal structures of the C-terminal domain (FliG-C) at 2.3 Å[19], a larger one containing the middle and C-terminal domain (FliG-MC) at 2.8 Å[20] at as well as the mutant FliG-MC at 2.3 Å[21], and the full-length FliG at 2.4 Å[22] have been resolved. However, virtually no structural information at the atomic level is known for PomA/PomB or the H^+ conducting stator unit MotA/MotB, except for the periplasmic PGB domain of the B subunit[23,24].

Blair and coworkers have previously directly shown the interaction between MotA and FliG by co-isolation assays[25,26]. Further, they have demonstrated that the electrostatic interaction between conserved charged residues in the cytoplasmic loop of MotA and the C-terminal region of FliG is important for the torque generation[26,27]. They concluded that several charged residues, Arg90 and Glu98 in MotA, and Lys264, Arg281, Glu288, Glu289 and Arg297 in FliG, are involved in the interaction, and they hypothesized

Table 1 Bacterial strains and plasmids used in this study

Strain or plasmid	Genotype or Description	Source or reference
E. coli strains		
DH5a	F⁻|*recA1 hsdR17 endA1 supE44 thi-1 relA1 gyrA96 Δ*(*argF-lacZYA*)U169 ϕ80Δ*lacZD*M15	
BL21	F⁻ *ompT hsdS* (*rB⁻ mB⁻*) *gal*	Novagen
RP6894	*ΔmotAB*	J. S. Parkinson
Plasmids		
pET30-GBFusion1	GB1 in pET30	PlasmID
pYS13	pomA and potB in pMMB206	40
pGB1/pCold	GB1 in pCold I	this study
pGB1-Aloop/pCold	GB1-PomAloop in pCold I	this study
pGB1/pBAD	GB1 in pBAD24	this study
pGB1-Aloop/pBAD	GB1-PomAloop in pBAD24	this study

that electrostatic interactions between the MotA-Loop and FliG are essential for their interactions and the motor rotation. Recently it has been suggested that the electrostatic interaction of MotA-Loop with FliG is required for the efficient assembly of the stators around the rotor[28,29].

On the other hand, in the Na^+-driven motor, site-directed substitutions of the corresponding charged residues of PomA and FliG as well as non-conserved neighboring charged residues do not affect the torque generation[30–32]. Furthermore, when charged mutations of PomA and FliG are combined and mutant proteins are expressed and assayed in *E. coli* using chimeric stator complexes, some of them showed patterns of synergism and suppression in rotor/stator double mutants similar to the *E. coli* motor, while others were ambiguous and did not show a clear-cut phenotype[33]. The sum of those observations suggests that electrostatic interactions are not always required for the rotation of the Na^+-driven flagellar motor or that different charged residues are present in the Na^+-driven flagellar motor. It has been suggested that interactions between the C-terminal domain of FliG and the cytoplasmic loop of PomA induce a structural change of PomB required for the proper assembly of PomA/PomB stator complexes around the rotor. We have attempted to detect interactions between PomA and FliG similar to MotA and FliG, but FliG does not co-isolate with PomA. Thus the molecular mechanism(s) of the stator-rotor interaction and its structural changes is still an open question, especially for the Na^+-driven motor.

In this study, to investigate the interactions of the rotor-stator interface, we cloned the cytoplasmic loop of PomA between the 2nd and 3rd transmembrane domains (the PomA-Loop). We purified the PomA-Loop fused with GB1 and characterized its biochemical features.

Materials and methods

Bacterial strains, media, plasmids and growth conditions

The strains and plasmids used are shown in Table 1. *E. coli* cells were cultured at 37°C in LB medium (1% Bacto tryptone, 0.5% yeast extract and 0.5% NaCl), at 30°C in TG medium (1% Bacto tryptone, 0.5% NaCl and 0.5% glycerol). When necessary, ampicillin and chloramphenicol were added to final concentrations of 50 μg/ml and 2.5 μg/ml, respectively. If necessary, L-arabinose was added to a final concentration of 0.02% (w/v).

Routine DNA manipulations were carried out according to standard procedures. The gene encoding the GB-1 protein tag (56 a.a., 6 kDa) was obtained from PlasmID (http://plasmid.med.harvard.edu/PLASMID/). The genes for PomA-Loop and GB1 were amplified using PCR from plasmids encoding wild-type PomA and GB1, respectively. The forward primer 5′-ACGGATCCCAGTTTTTTGGTGCGACAAAG-3′ and the reverse primer 5′-CTGGTACCTTAGTCGCCAAA GGCGCGAAATACACC-3′ were designed for the PomA-Loop (underlining indicates restriction sites for *BamH*I and *Kpn*I, respectively). The forward universal primer (T7 promoter) and the reverse universal primer (T7 terminator) were used for the extension of GB1. These fragments were digested by NdeI and BamHI for the PCR product of GB1 and by BamHI and KpnI for the PCR product of the PomA-Loop, and the digested fragments were ligated to the *Nde*I and *Kpn*I sites of the pCold-I vector (TAKARA BIO, Inc., Otsu, Japan). Consequently, the plasmid encodes 6 histidines at the N-terminus, and it was named pGB1-Aloop/pCold. This cloning strategy resulted in the following N- and C-terminal peptide sequences: MNHKVHHHHHH---$^{1(GB1)}$ MQYK---GSQ$^{54(PomA)}$FF---FGD$^{148(PomA)}$. The forward primer 5′-GGCCATGGTGCATCATCATCATCATC-3′ and the reverse primer 5′-GGCAGGGATCTTAGATTCTG-3′ were used for extensions of the GB1-Aloop from pGB1-Aloop/pCold (underlining indicates the restriction site for NcoI). The fragment was digested by NcoI and HindIII for the PCR product GB1-Aloop, and the digested fragment was ligated to the NcoI and HindIII sites of the pBAD24 vector. This plasmid was named pGB1-Aloop/pBAD24. The constructed plasmids were analyzed using an automated sequencer to confirm the expected nucleotide sequences.

Protein expression and purification

Cells were grown in LB medium supplemented with ampicillin (final concentration of 50 μg/ml). *E. coli* BL21 cells harboring plasmids were grown at 16°C for 16 hr with

0.5 mM IPTG for pGB1/pCold and pGB1-Aloop/pCold. Cells were harvested by centrifugation and were resuspended in buffer containing 50 mM Tris-Cl (pH 8.0) supplemented with a protease inhibitor tablet (Sigma Chemical Co., St. Louis, MO). Thawed cells were disrupted by sonication on ice. Crude membranes were collected by centrifugation (22,300×*g* for 30 min at 4°C), and the resultant supernatant was applied to a Ni-affinity column (HisTrap, GE Healthcare, Uppsala, Sweden) at 4°C. The column was then washed extensively with buffer containing 500 mM NaCl, 20 mM imidazole and 50 mM Tris-Cl (pH 8.0) to remove unspecifically bound proteins. The histidine-tagged proteins were then eluted using an imidazole gradient. The eluted samples were further purified by an ion exchange column (HiTrap Q, GE Healthcare) and a gel-filtration column, Superdex 200HR (GE Healthcare) in buffer containing 50 mM Tris-Cl (pH 8.0).

Swiming assay

Aliquots (1 μL) of overnight cultures in TG medium were spotted onto TG plates containing 0.3% agar, 50 μg/ml ampicillin and 2.5 μg/ml chloramphenicol and were incubated at 30°C.

Measurement of swimming speed

Overnight cultures in TG medium were inoculated into TG medium at a 100-fold dilution. When the expression plasmids used the pBAD vector, the cells were cultivated for 3 hours with 0.02% arabinose and 0.1 mM IPTG. Cells were diluted 50-fold into TG medium and were observed using dark-field microscopy. Images of the cells were recorded on a video recorder, and the swimming speeds of the cells were measured using software for motion analysis (Move-tr/2D, Library Co., Tokyo).

Detection of PomA by immunoblotting

Samples were dissolved in sodium dodecyl sulfate-polyacrylamide gel electrophoresis (SDS-PAGE) loading buffer containing 5% 2-mercaptoethanol and were separated by 15%-acrylamide SDS-PAGE. Immunoblotting was performed using an anti-PomA antibody (PomA91).

Analytical size exclusion column chromatography

Analytical size exclusion chromatography was performed with a Superdex 200 HR 10/300 column (GE Healthcare) connected to an AKTA system (GE Healthcare). The column was equilibrated with buffer containing 50 mM Tris-Cl (pH 8.0) and was eluted at a flow rate of 0.5 ml/min. A high molecular weight standard solution (GE Healthcare) was used for size markers.

Circular dichroism (CD) spectroscopy

The CD spectrum was recorded on a JASCO (Tokyo, Japan) J-720W CD spectropolarimeter at room temperature between 250 and 200 nm (0.1 cm cell) at 0.2 nm intervals with a scan speed of 10 nm/min. Signals were averaged over 8 separate scans. The protein concentration was 25 μg/ml in a buffer solution containing 50 mM Tris-Cl (pH 8.0).

Differential scanning calorimetry (DSC)

Before the DSC experiments, the samples were dialyzed against 50 mM potassium phosphate buffer (pH 8.0). The dialysate buffer was used as a reference solution for the DSC scan. Both calorimetric scans were performed using NanoDSC (TA Instruments, Inc., New Castle, DE). GB1-Aloop (1 mg/ml) was scanned from 15 to 90°C, with a heating rate of 1°C/min.

NMR spectroscopy

Uniformly ^{15}N-labeled proteins for NMR experiments were prepared by growing cells harboring the pGB1-Aloop/pCold plasmid in standard minimal medium (M9) containing 0.5 g/l ^{15}N-ammonium chloride (Isotec Inc., Miamisburg, OH). Transformed cells were initially grown at 37°C in 100 ml of the isotope-labeled M9 medium and were inoculated directly into 900 ml of the medium. The cells were grown at 16°C for 48 hr with 0.1 mM IPTG.

Samples were concentrated and exchanged using an Amicon Ultra filter (Millipore, Bedford, MA) against media whose compositions are described below. NMR experiments were performed at 283 K on a Bruker Avance 500 spectrometer with a [^{1}H/^{15}N] pulse field gradient cryogenic probe in a buffer solution containing 50 mM Tris-Cl (pH 6.8) and 200 mM NaCl. All data were processed using the NMRPipe program and were analyzed using the Sparky (http://www.cgl.ucsf.edu/home/sparky/) program. To estimate the binding affinity, intensity changes were obtained by cognate peak height (initial=0).

Results

Protein expression and purification

PomA has four transmembrane regions with a large cytoplasmic loop (PomA-Loop) between the 2nd and 3rd transmembrane region (Fig. 1A). It has been proposed that in *E. coli* the large cytoplasmic loop of MotA is important for its interaction with FliG. In general, it is not easy to express membrane proteins, and in fact, the expression level of full-length PomA was low in the *E. coli* expression system. Therefore, we tried to express the 10.4 kDa PomA-Loop (94 a.a. from Q54 to D148) with a His-tag added at the N-terminus. Figure 1B shows the SDS-PAGE patterns of the PomA-Loop stained with Coomassie Brilliant Blue (CBB, A-loop), and western blotting analysis using an anti-PomA antibody (IB). The total cell lysate of *E. coli* expressing the PomA-Loop (T) was centrifuged at 22,300×*g* for 30 min to separate the insoluble fraction (I) from the soluble fraction (S). The PomA-Loop (A-loop) was harvested from the insoluble fraction, suggesting that the protein forms an inclusion body. Therefore, the insoluble proteins were solubi-

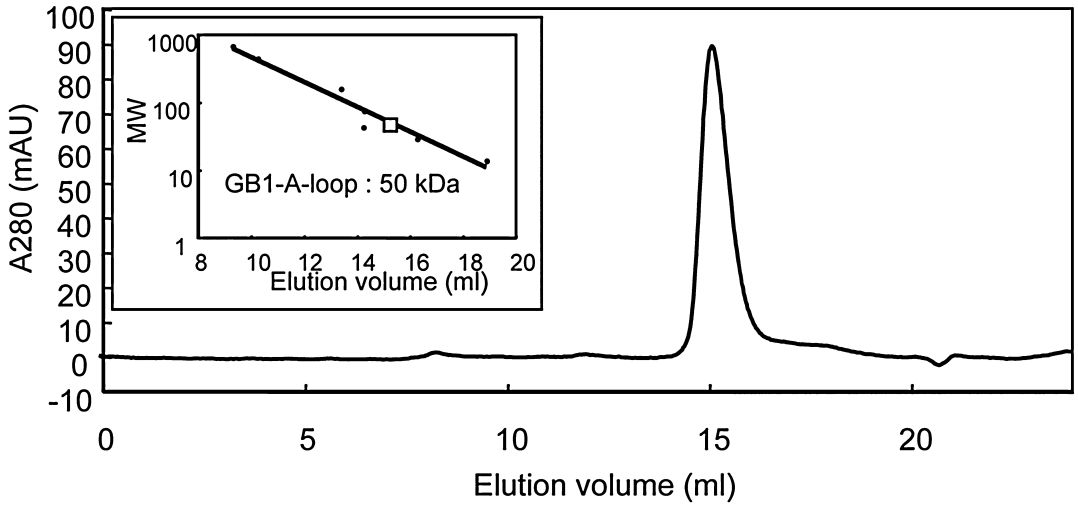

Figure 2 Analytical gel-filtration of the GB1-PomA-Loop. Elution profiles of the purified GB1-PomA-Loop (peak at 15.1 ml) determined by analytical size exclusion chromatography with a Superdex 200 HR 10/300 column. Inset indicates the elution patterns of the size marker proteins Thyroglobin (669 kDa), Ferritin (440 kDa), Aldolase (158 kDa), Conalbumin (75 kDa), Ovalbumin (43 kDa), Carbonic anhydrolase (29 kDa) and Ribonuclease A (13.7 kDa) at 9.3 ml, 10.2 ml, 13.4 ml, 14.2 ml, 14.2 ml, 16.2 ml and 18.9 ml, respectively. OD280, optical density at 280 nm; mAU, milliabsorbance units.

lized using a buffer containing 8 M urea, and the sample was then applied to a Ni-NTA column. The sample was refolded successfully as a soluble protein by an on-column refolding method by gently removing the urea. However, the proteins formed a precipitate within a few hours (data not shown). It is well known that soluble-tags, such as MBP and NUS, are very useful to solubilize insoluble proteins[34]. Here, the PomA-Loop was fused with a small soluble tag, GB1[35], and a His tag at the N-terminus. The molecular weight of the resultant fusion protein is ca. 19 kDa. Figure 1B shows the SDS-PAGE patterns of the PomA-Loop fused with GB1 stained with Coomassie Brilliant Blue (CBB, GB1-A-loop), and western blotting analysis using an anti-PomA antibody (IB). Fortunately, the fusion was harvested mainly in the soluble fraction, and could be purified using a Ni^{2+}-affinity column and an ion exchange column, Hitrap Q (P of Fig. 1B). Thus, the PomA-Loop could be prepared in good yield with high quality as a fusion protein (15 mg/L culture). This is the first report that the PomA protein can be over-produced in a soluble form.

As shown in Figure 2, only one sharp peak exhibiting high symmetry at a volume of 15.1 ml was eluted by analytical size exclusion chromatography with a Superdex 200 HR 10/300 column. This indicates that the GB1-PomA-loop exists as a single species in solution and was estimated as a 50 kDa protein, indicating that the size of the PomA-Loop with GB1 in solution is much larger than the deduced size of the PomA-Loop with the GB1 monomer (19 kDa).

Characterization of the recombinant GB1-PomA-Loop

At first we investigated whether the recombinant PomA-loop with GB1 has a folded secondary structure using far-UV circular dichroism (CD) spectra (Fig. 3A). Tetrahydrofuran (THF) was used as an inducer of protein folding. There was almost no effect of THF (2.5% w/v) for the GB1-PomA-loop (data not shown). The negative peak at ~222 nm that is a typical signal for an α-helix was observed in the GB1-PomA-Loop. CD spectroscopy indicated that the PomA-Loop with GB1 and GB1 only was composed of ca. 14% and 26% α-helix, ca. 39% and 47% β-sheet, and ca. 37% and 24% random structures, respectively (estimated using software from JASCO) (Fig. 3A). This suggests that most of the A loop region might not have a specific structure because the α-helix content is decreased and the random structure is increased in PomA-Loop.

As for the three-dimensional structure of the recombinant PomA-Loop with GB1, DSC experiments were performed. The DSC curve of the GB1-PomA-Loop exhibited a peak of excess heat capacity at 67°C in 50 mM phosphate buffer (pH 8.0) (Fig. 3B). The heat denaturation of the GB1-PomA-loop was irreversible. The specific denaturation enthalpy change (ΔH) of the protein, 16.5 J/g, was an appropriate value for many folded proteins (between 10 and 27 J/g). This curve profile is in good agreement with a fitting curve assumed by the two-state transition model. The profile of GB1 only is almost the same as the profile of the GB1-PomA-loop. This suggests that the ΔH of the recombinant protein of the GB1-PomA-loop is derived only from GB1 but not from the loop region. This also supports that most of the A loop region may not have a specific structure.

Figure 3C shows a ^{1}H-^{15}N two-dimensional HSQC NMR spectrum of 0.1 mM GB1 alone and 0.1 mM GB1-PomA-Loop in 50 mM Tris-Cl (pH 6.8), 200 mM NaCl at 283 K. The spectrum of GB1 alone is essentially the same as that of the previous report. The cross-peaks of GB1 alone (colored red) coincide well with those of the GB1-PomA-Loop (col-

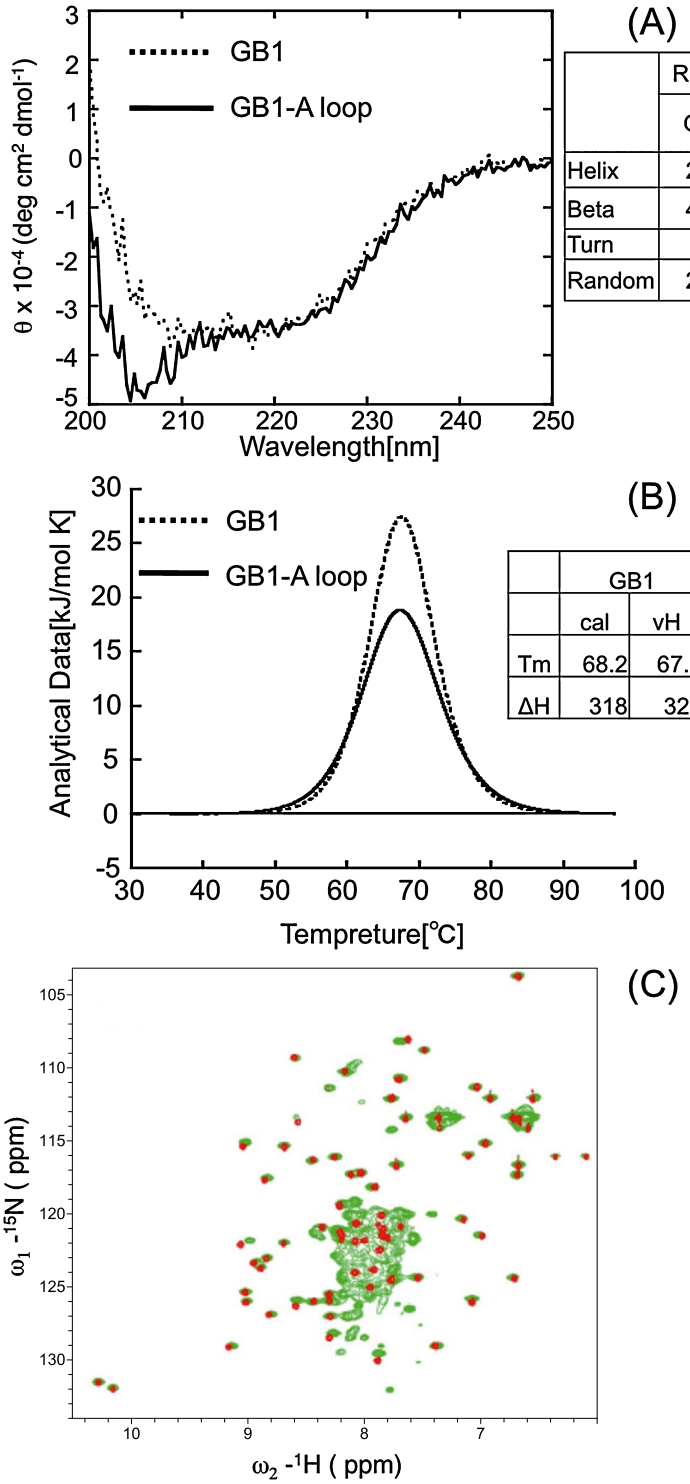

	Relative amount	
	GB1	GB1-A loop
Helix	25.8%	13.5%
Beta	47.4%	39.2%
Turn	3.0%	10.7%
Random	23.8%	36.5%

	GB1		GB1-A loop	
	cal	vH	cal	vH
Tm	68.2	67.7	67.4	67.5
ΔH	318	322	266	270

Figure 3 Characterization of the GB1-A-loop. (A) Far-UV CD spectrum of the GB1-PomA-Loop with GB1. The protein concentration was 25 μg/ml in a buffer solution containing 50 mM Tris-Cl (pH 8.0). The structural compositions (the table on the right side) are estimated using software from JASCO. The percentages of the structures for α-helix, β-strand, turn, and random are shown in the table on the right. (B) DSC profiles of the GB1-A-loop and GB1. The protein concentration was 1 mg/ml in a buffer solution containing 50 mM phosphate buffer (pH 8.0). The data were analyzed using NanoAnalyze software (TA Instruments, Japan). The resulting thermogram and the fitting data are shown in a dotted line for GB1 and in a line for the GB1-A-loop. The estimated values of specific denaturation enthalpy change (ΔH) and peak of excess heat capacity (Tm). (C) NMR experiments are shown in the table on the right. Two-dimensional ^{1}H-^{15}N HSQC spectra of GB1 alone (red) and the GB1-PomA-Loop (green). The protein concentrations were 0.1 mM for GB1 and 0.1 mM for GB1-PomA-Loop.

ored green), indicating that the protein conformation of GB1 is not affected by the PomA-Loop, and vice versa. In addition, the peaks of GB1-PomA-Loop except for the peaks originating from the GB1 are tentatively assigned as the resonances from the PomA-Loop.

Dominant negative effect of the GB1-PomA-Loop on motility

Blair and coworkers have identified many point mutations in *E. coli motA* that give a Mot$^-$ (paralyzed flagella) phenotype[36,37]. Those mutations are located within the large cytoplasmic loop of MotA, and include the charged residues. Those mutant variants also exhibit a dominant negative effect on the motility of the wild-type, which probably reflects the displacement of functional MotA by the nonfunctional protein. Furthermore, Morimoto *et al.* have reported that the over-expression of MotA alone considerably inhibits motility of *Salmonella* wild-type cells and this was explained by the reduction in the number of functional stators[28]. To investigate whether the PomA-Loop shows a similar effect, we introduced the PomA-Loop with GB1 into cells expressing the PomA/PotB complex. PotB is a chimeric protein consisting of the N-terminal PomB fused to the C-terminal MotB, and complexed with PomA, that works as the stator of the Na^+-driven flagellar motor in *E. coli*. Figure 4A shows the swarming abilities of *E. coli* RP6894 (Δ*motAB*) expressing GB1 (GB1), GB1-PomA-Loop (GB1-A), GB1 with PomA/PotB (GB1, PomAPotB), and GB1-PomA-Loop with PomA/PotB (GB1-A, PomAPotB) in the absence (upper plate) or presence of 0.02% arabinose (lower plate). The swimming speeds of cells expressing GB1 or the GB1-PomA-Loop with PomA/PotB were measured in the presence of 0.02% arabinose. When the GB1-PomA-Loop was expressed in the PomA/PotB background, the swimming ability in soft agar and swimming speed was impaired reproducibly although the effects were not drastic (Fig. 4A and B). Thus, these data suggest that the GB1-PomA-Loop gives a dominant negative effect against the wild-type PomA protein. It should be noted that the tumbling frequency of cells expressing the GB1-PomA-Loop was almost identical to that of GB1, indicating there was no effect on the chemotactic signal transduction pathway.

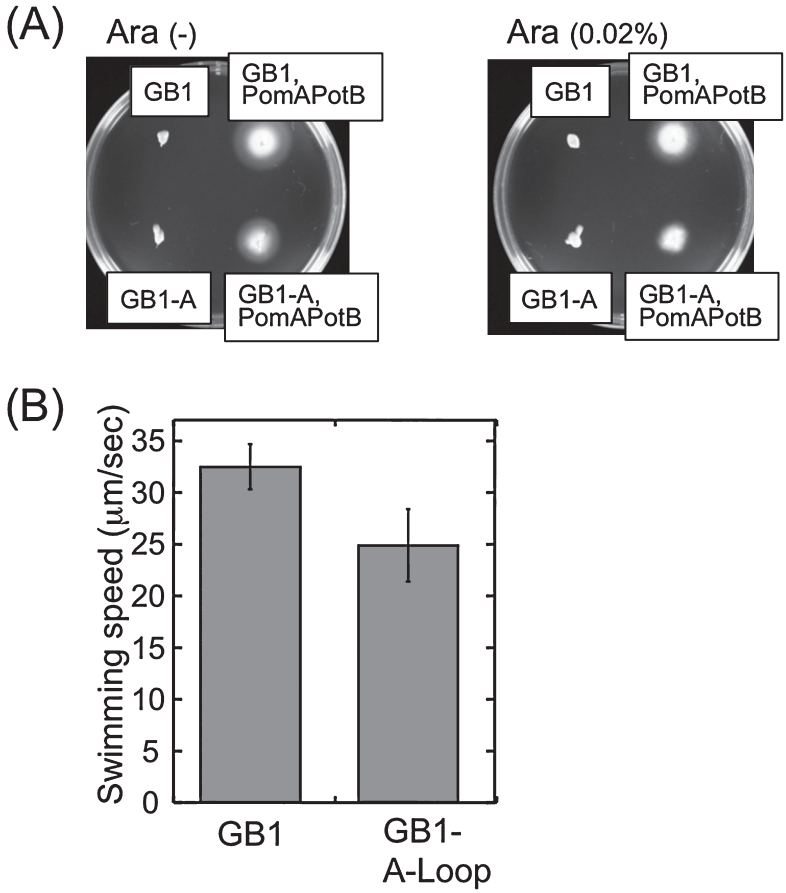

Figure 4 Dominant properties of the PomA-Loop. (A) Swarming motility assay of *E. coli* RP6894 transformed with plasmids encoding GB1 or the GB1-PomA-Loop (GB1-A) with PomA and PotB. Cells were inoculated in soft-agar plates with or without 0.02% arabinose for pGB1/pBAD24 and pGB1-Aloop/pBAD24. Plates were incubated at 30°C for 8 h for cells having pBAD vectors. (B) Swimming of RP6894 cells transformed with plasmids encoding GB1 or the GB1-PomA-Loop (GB1-A) with PomA and PotB. The swimming speeds were determined from at least 200 individual cells and three independent measurements.

Discussion

Flagellar motor proteins participate in energy transduction from electrochemical potential to a mechanical output, i.e. the rotation of the flagellum. The PomA/PomB complex works as the stator and ion conductor in the Na^+-driven flagellar motor in *V. alginolyticus*. An initial model of $MotA_4MotB_2$ ($PomA_4PomB_2$) organization has been proposed, in which a dimer of MotB transmembrane domains is located at the center of the complex[3]. Transmembrane domains 3 (TM3) and 4 (TM4) of the four MotA molecules are arranged in the inner layer around the MotB segments, and TM1 and TM2 are located on the outside. Thus, TM3 and TM4 of MotA (PomA) are in close proximity to the TM domain of MotB (PomB)[38,39]. Where and how does the stator recognize the coupling ion and generate the torque in the stator complex? It is believed that the energy of the ion flux is converted into structural changes of the PomA/PomB complex which result in the conformational changes of the rotor protein, FliG. To test that hypothesis, it is essential to directly detect the rotor-stator interactions.

In this study, we cloned the large cytoplasmic loop of PomA and over-expressed it in *E. coli*. The protein could be isolated as an insoluble form. The insoluble protein could be solubilized by urea but it precipitated when the urea was removed. Thus, we used a soluble-tag, GB1, and the 19 kDa fusion protein could be purified as a soluble recombinant protein (Fig. 2). The estimated molecular weight by size exclusion chromatography was ca. 50 kDa. This size is much larger than the size predicted from the amino acid sequence of the PomA-Loop with GB1 and the molecular mass estimated by SDS-PAGE. This might indicate that the fusion protein forms a dimer, or that the structure of the fusion protein is very elongated or that its tertiary structure is loose. The CD spectral data and the DSC curve suggest that both of their structures might not have a specific structure in solution (Fig. 3). However, the PomA-Loop shows a slight dominant negative effect on the motility of cells expressing the PomA/PotB complex (Fig. 4), which reflects the competition of functional PomA by a nonfunctional fragment or the completion against FliG to reduce the number of functional stators. We think that the loop alone retains a certain function. The conformational changes can be regenerated repeatedly by the torque generation induced by Na^+ flux through the PomA/PomB stator complex. Using those recombinant proteins, we will try to detect the direct interaction between the cytoplasmic region of PomA and FliG *in vitro*.

Acknowledgements

This work was supported in part by grants-in-aid for scientific research from the Ministry of Education, Science, and Culture of Japan; the Japan Science and Technology Corporation (to M.H., Y.S., C.K. and S.K.).

References

1. Macnab, R.M. How bacteria assemble flagella. *Annu. Rev. Microbiol.* **57**, 77–100 (2003).
2. Berg, H.C. The rotary motor of bacterial flagella. *Annu. Rev. Biochem.* **72**, 19–54 (2003).
3. Blair, D.F. Flagellar movement driven by proton translocation. *FEBS Lett.* **545**, 86–95 (2003).
4. Li, N., Kojima, S. & Homma, M. Sodium-driven motor of the polar flagellum in marine bacteria *Vibrio*. *Genes Cells* **16**, 985–999 (2011).
5. Terashima, H., Kojima, S. & Homma, M. Flagellar motility in bacteria structure and function of flagellar motor. *Int. Rev. Cell Mol. Biol.* **270**, 39–85(2008).
6. Kojima, S. & Blair, D.F. The bacterial flagellar motor: structure and function of a complex molecular machine. *Int. Rev. Cytol.* **233**, 93–134 (2004).
7. Asai, Y., Kojima, S., Kato, H., Nishioka, N., Kawagishi, I. & Homma, M. Putative channel components for the fast-rotating sodium-driven flagellar motor of a marine bacterium. *J. Bacteriol.* **179**, 5104–5110 (1997).
8. Chun, S.Y. & Parkinson, J.S. Bacterial motility: membrane topology of the *Escherichia coli* MotB protein. *Science* **239**, 276–278 (1988).
9. Zhou, J., Fazzio, R.T. & Blair, D.F. Membrane topology of the MotA protein of *Escherichia coli*. *J. Mol. Biol.* **251**, 237–242 (1995).
10. Sato, K. & Homma, M. Functional reconstitution of the Na^+-driven polar flagellar motor component of *Vibrio alginolyticus*. *J. Biol. Chem.* **275**, 5718–5722 (2000).
11. Zhou, J., Sharp, L.L., Tang, H.L., Lloyd, S.A., Billings, S., Braun, T.F. & Blair, D.F. Function of protonatable residues in the flagellar motor of *Escherichia coli*: a critical role for Asp 32 of MotB. *J. Bacteriol.* **180**, 2729–2735 (1998).
12. Sudo, Y., Terashima, H., Abe-Yoshizumi, R., Kojima, S. & Homma, M. Comparative study of the ion flux pathway in stator units of proton- and sodium-driven flagellar motors. *Biophysics* **5**, 45–52 (2009).
13. Obara, M., Yakushi, T., Kojima, S. & Homma, M. Roles of charged residues in the C-terminal region of PomA, a stator component of the Na^+-driven flagellar motor. *J. Bacteriol.* **190**, 3565–3571 (2008)..
14. Kojima, S. & Blair, D.F. Conformational change in the stator of the bacterial flagellar motor. *Biochemistry* **40**, 13041–13050 (2001).
15. Irikura, V.M., Kihara, M., Yamaguchi, S., Sockett, H. & Macnab, R.M. *Salmonella typhimurium fliG* and *fliN* mutations causing defects in assembly, rotation, and switching of the flagellar motor. *J. Bacteriol.* **175**, 802–810 (1993).
16. Lloyd, S.A., Tang, H., Wang, X., Billings, S. & Blair, D.F. Torque generation in the flagellar motor of *Escherichia coli*: evidence of a direct role for FliG but not for FliM or FliN. *J. Bacteriol.* **178**, 223–231 (1996).
17. Thomas, D.R., Francis, N.R., Xu, C. & DeRosier, D.J. The three-dimensional structure of the flagellar rotor from a clockwise-locked mutant of *Salmonella enterica* serovar Typhimurium. *J. Bacteriol.* **188**, 7039–7048 (2006).
18. Liu, J., Lin, T., Botkin, D.J., McCrum, E., Winkler, H. & Norris, S.J. Intact flagellar motor of Borrelia burgdorferi revealed by cryo-electron tomography: evidence for stator ring curvature and rotor/C-ring assembly flexion. *J. Bacteriol.* **191**, 5026–5036 (2009).
19. Lloyd, S.A., Whitby, F.G., Blair, D.F. & Hill, C.P. Structure of the C-terminal domain of FliG, a component of the rotor in the bacterial flagellar motor. *Nature* **400**, 472–475 (1999).

20. Brown, P. N., Hill, C. P. & Blair, D. F. Crystal structure of the middle and C-terminal domains of the flagellar rotor protein FliG. *EMBO J.* **21**, 3225–3234 (2002).
21. Minamino, T., Imada, K., Kinoshita, M., Nakamura, S., Morimoto, Y. V. & Namba, K. Structural insight into the rotational switching mechanism of the bacterial fagellar motor. *PLoS Biol.* **9**, e1000616 (2011).
22. Lee, L. K., Ginsburg, M. A., Crovace, C., Donohoe, M. & Stock, D. Structure of the torque ring of the flagellar motor and the molecular basis for rotational switching. *Nature* **466**, 996–1000 (2010).
23. Roujeinikova, A. Crystal structure of the cell wall anchor domain of MotB, a stator component of the bacterial flagellar motor: implications for peptidoglycan recognition. *Proc. Natl. Acad. Sci. USA* **105**, 10348–10353 (2008).
24. Kojima, S., Imada, K., Sakuma, M., Sudo, Y., Kojima, C., Minamino, T., Homma, M. & Namba, K. Stator assembly and activation mechanism of the flagellar motor by the periplasmic region of MotB. *Mol. Microbiol.* **73**, 710–718 (2009).
25. Tang, H., Braun, T. F. & Blair, D. F. Motility protein complexes in the bacterial flagellar motor. *J. Mol. Biol.* **261**, 209–221 (1996).
26. Zhou, J., Lloyd, S. A. & Blair, D. F. Electrostatic interactions between rotor and stator in the bacterial flagellar motor. *Proc. Natl. Acad. Sci. USA* **95**, 6436–6441 (1998).
27. Lloyd, S. A. & Blair, D. F. Charged residues of the rotor protein FliG essential for torque generation in the flagellar motor of *Escherichia coli*. *J. Mol. Biol.* **266**, 733–744 (1997).
28. Morimoto, Y.V., Nakamura, S., Kami-ike, N., Namba, K. & Minamino, T. Charged residues in the cytoplasmic loop of MotA are required for stator assembly into the bacterial flagellar motor. *Mol. Microbiol.* **78**, 1117–1129 (2010).
29. Morimoto, Y. V., Nakamura, S., Hiraoka, K. D., Namba, K. & Minamino, T. Distinct roles of highly conserved charged residues at the MotA-FliG interface in bacterial flagellar motor rotation. *J. Bacteriol.* **195**, 474–481 (2013).
30. Yorimitsu, T., Mimaki, A., Yakushi, T. & Homma, M. The conserved charged residues of the C-terminal region of FliG, a rotor component of the Na^+-driven flagellar motor. *J. Mol. Biol.* **334**, 567–583 (2003).
31. Yorimitsu, T., Sowa, Y., Ishijima, A., Yakushi, T. & Homma, M. The systematic substitutions around the conserved charged residues of the cytoplasmic loop of Na^+-driven flagellar motor component PomA. *J. Mol. Biol.* **320**, 403–413 (2002).
32. Fukuoka, H., Yakushi, T. & Homma, M. Concerted effects of amino acid substitutions in conserved charged residues and other residues in the cytoplasmic domain of PomA, a stator component of Na^+-driven flagella. *J. Bacteriol.* **186**, 6749–6758 (2004).
33. Yakushi, T., Yang, J., Fukuoka, H., Homma, M. & Blair, D. F. Roles of charged residues of rotor and stator in flagellar rotation: comparative study using H^+-driven and Na^+-driven motors in *Escherichia coli*. *J. Bacteriol.* **188**, 1466–1472 (2006).
34. Terpe, K. Overview of tag protein fusions: from molecular and biochemical fundamentals to commercial systems. *Appl. Microbiol. Biotechnol.* **60**, 523–533 (2003).
35. Zhou, P., Lugovskoy, A. A. & Wagner, G. A solubility-enhancement tag (SET) for NMR studies of poorly behaving proteins. *J. Biomol. NMR* **20**, 11–14 (2001).
36. Zhou, J. & Blair, D. F. Residues of the cytoplasmic domain of MotA essential for torque generation in the bacterial flagellar motor. *J. Mol. Biol.* **273**, 428–439 (1997).
37. Braun, T. F., Poulson, S., Gully, J. B., Empey, J. C., Van Way, S., Putnam, A. & Blair, D. F. Function of proline residues of MotA in torque generation by the flagellar motor of *Escherichia coli*. *J. Bacteriol.* **181**, 3542–3551 (1999).
38. Kim, E. A., Price-Carter, M., Carlquist, W. C. & Blair, D. F. Membrane segment organization in the stator complex of the flagellar motor: implications for proton flow and proton-induced conformational change. *Biochemistry* **47**, 11332–11339 (2008).
39. Kojima, S. & Blair, D. F. Solubilization and purification of the MotA/MotB complex of *Escherichia coli*. *Biochemistry* **43**, 26–34 (2004).
40. Sowa, Y., Rowe, A. D., Leake, M. C., Yakushi, T., Homma, M., Ishijima, A. & Berry, R. M. Direct observation of steps in rotation of the bacterial flagellar motor. *Nature* **437**, 916–919 (2005).